

Tailoring magnetic vortices in nanostructures

F. Garcia, H. Westfahl, J. Schoenmaker, E. J. Carvalho, A. D. Santos et al.

Citation: *Appl. Phys. Lett.* **97**, 022501 (2010); doi: 10.1063/1.3462305

View online: <http://dx.doi.org/10.1063/1.3462305>

View Table of Contents: <http://apl.aip.org/resource/1/APPLAB/v97/i2>

Published by the [American Institute of Physics](#).

Related Articles

The magneto-optical behaviors modulated by unaggregated system for γ -Fe₂O₃-ZnFe₂O₄ binary ferrofluids
[AIP Advances 2, 042124 \(2012\)](#)

Magnetization states of a spin-torque oscillator having perpendicular polarizer and planar free layer
[J. Appl. Phys. 112, 083926 \(2012\)](#)

Magnetic and electrical properties of In doped cobalt ferrite nanoparticles
[J. Appl. Phys. 112, 084321 \(2012\)](#)

Effective magnetic anisotropy of annealed FePt nanoparticles
[Appl. Phys. Lett. 101, 172402 \(2012\)](#)

Perpendicular magnetic anisotropy in Nd-Co alloy films nanostructured by di-block copolymer templates
[J. Appl. Phys. 112, 083914 \(2012\)](#)

Additional information on Appl. Phys. Lett.

Journal Homepage: <http://apl.aip.org/>

Journal Information: http://apl.aip.org/about/about_the_journal

Top downloads: http://apl.aip.org/features/most_downloaded

Information for Authors: <http://apl.aip.org/authors>

ADVERTISEMENT

**Universal charged-particle detector
for interdisciplinary applications:**

- > Non-scanning Mass Spectrometry
- > Non-scanning Ion Mobility Spectrometry
- > Non-scanning Electron Spectroscopy
- > Direct microchannel plate readout
- > Thermal ion motion and mobility studies
- > Bio-molecular ion soft-landing profiling
- > Real-time beam current/shape tuning
- > Diagnostics tool for instrument design
- > Compact linear array for beam lines

Contact OI Analytical: +1-205-733-6900

The advertisement features a 3D perspective of a detector chip with a color gradient from yellow to purple. Text on the chip includes: 'Thermal hyper-thermal keV-energy ions', 'Atmospheric Pressure to Ultra High Vacuum', 'IonCCD™ for charged particles', '24µm spatial resolution (2136 pixels)', and '3ns temporal resolution (360 fps)'. The OI Analytical logo is in the top right corner.

Tailoring magnetic vortices in nanostructures

F. Garcia,^{1,a)} H. Westfahl,¹ J. Schoenmaker,¹ E. J. Carvalho,¹ A. D. Santos,² M. Pojar,³ A. C. Seabra,³ R. Belkhou,^{4,5} A. Bendounan,⁴ E. R. P. Novais,⁶ and A. P. Guimarães⁶

¹Laboratório Nacional de Luz Síncrotron, Campinas, 13083-970 São Paulo, Brazil

²LMM, IFUSP, São Paulo, 05508-900 São Paulo, Brazil

³LSI-PSI, Poli-USP, São Paulo, 05508-900 São Paulo, Brazil

⁴Synchrotron SOLEIL, F-91192 Gif-sur-Yvette Cedex, France

⁵Elettra Sincrotron, 34149 Trieste, Italy

⁶CBPF, Rio de Janeiro, 22290-180 Rio de Janeiro, Brazil

(Received 5 March 2010; accepted 18 June 2010; published online 12 July 2010)

Tailoring the properties of magnetic vortices through the preparation of structured multilayers is discussed. The dependence of the vortex core radius r on the effective anisotropy is derived within a simple model, which agrees with our simulations. As the perpendicular anisotropy increases, r also increases until a perpendicular magnetization appears in the disk rim. Co/Pt multilayer disks were studied; x-ray microscopy confirms qualitatively the predicted behavior. This is a favorable system for implementing vortex-based spin-transfer nano-oscillator devices, with enhanced rf power resulting both from the increase in the core size and synchronization afforded by the coupling of the Co layers. © 2010 American Institute of Physics. [doi:10.1063/1.3462305]

In nanomagnetic samples the magnetic domain configuration depends on several parameters of the system such as size, shape, anisotropy, magnetic exchange stiffness, interface roughness, etc. A magnetic vortex often represents the lowest energy configuration,¹ being characterized by the following features: polarity (up or down direction of the vortex core) and circulation (clockwise or counterclockwise curling direction). Vortices have drawn great interest among researchers dealing with nanostructured materials.² Their technological applications are numerous, encompassing from devices such as vortex random access memories^{3,4} to bio-functionalized microdisks for cancer treatment.⁵ They also represent a key system to understand magnetism in reduced dimensions; e.g., a vortex-antivortex square lattice was proposed as a laboratory system for the study as an analog to the Bose–Einstein condensation.⁶

Another application is vortex-based spin transfer nano-oscillators (VSTNOs), used as microwave generator devices and suitable for device integration.^{7–9} Despite their great appeal, these devices generate low power and dissipate much heat. It was demonstrated experimentally,⁶ that the microwave power can be increased through phase-locking of closely spaced nano-oscillators. Still lacking is optimizing the synchronization of these devices. To face these challenges, a fine engineering of the vortex features and optimizing device geometry is highly desirable. Many efforts have been made in order to modify the vortex properties,¹⁰ however, properties such as vortex core size are hard to adjust and highly dependent on the magnetic anisotropies of the system.¹¹

In Co/Pt multilayer systems the effective magnetic anisotropy (K_{eff}) is sensitive to the interface contributions, and can be easily controlled from in-plane to out-of-plane by playing with the Co thickness [e.g., see Ref. 12]. Moreover, these systems have been shown to present TMR or GMR.^{9,13–15} In this letter, we propose Co/Pt multilayer engi-

neering to tailor the Co vortex properties by means of the interface contribution to K_{eff} ; we show how the vortex core magnetization and radius (r) can be tailored by controlling K_{eff} .

According to studies on single-layered structures, typically vortices cores have $r \sim 5$ nm. In the limit of small thickness ($t \rightarrow 0$), r can be expressed by¹⁶ $\sqrt{A/K_d}$, where A is the exchange stiffness and K_d is the magnetostatic energy density ($K_d = \mu_0 M_s^2 / 2$). The effective anisotropy K_{eff} in Co/Pt multilayers can be described by the following phenomenological expression:

$$K_{\text{eff}} = K_v - 2(K_s/t), \quad (1)$$

where t is the Co thickness, K_v and K_s are the volume and interface anisotropy, respectively. From Eq. (1), one sees that it is possible to vary K_{eff} of a multilayer, simply by varying t ; as K_{eff} crosses zero, there is a spin reorientation, from in-plane ($K_{\text{eff}} > 0$) to out-of-plane ($K_{\text{eff}} < 0$).¹²

Following Ref. 16, we used the ansatz for the core magnetization of a vortex, in cylindrical coordinates; $m_z = m_z(\rho) = \exp(-2\beta^2\rho^2)$, where β is the variation parameter, corresponding to $1/2r$. We have considered no in-plane anisotropy, only perpendicular anisotropy energy, proportional to the perpendicular anisotropy constant K_z as follows:

$$E_z = -2\pi K_z t \int \rho d\rho m_z^2 = \pi K_z t \frac{[\exp(-4D^2\beta^2) - 1]}{4\beta^2}. \quad (2)$$

Minimizing the total energy, i.e., exchange, magnetostatic [Eqs. (5) and (8) of Refs. 16, respectively] and perpendicular anisotropy energy, we arrive at the following:

$$\frac{1}{\beta} = 2r = 2\sqrt{\frac{A}{K_d - K_z}}, \quad (3)$$

valid up to the limit r much smaller than the disk diameter D , i.e., $\beta D \gg 1$. Note that in this approximation r diverges for a sufficiently large anisotropy, and for $K_d < K_z$, there is no real solution.

^{a)}Electronic mail: fgarcia@lnls.br.

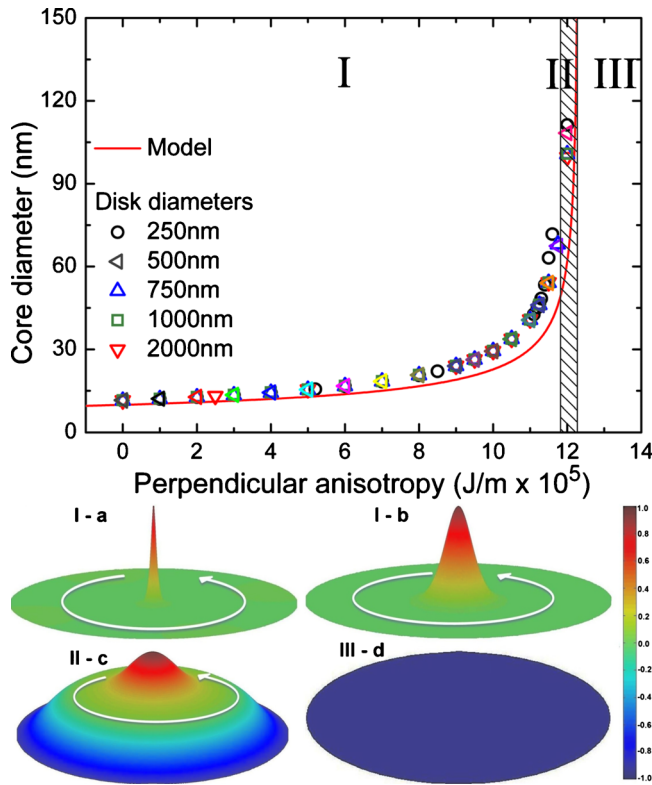


FIG. 1. (Color online) Simulated phase diagram of spin configuration of the Co/Pt multilayer disks as a function of perpendicular anisotropy and disk diameter. [a(i)] narrow core diameter ($K_z=0$). [b(i)] wide core diameter ($K_z=1.18 \times 10^5$ J/m³). [c(II)] annular spin structure ($K_z=1.2 \times 10^5$ J/m³). [d(III)] perpendicular single domain ($K_z > 1.2 \times 10^5$ J/m³).

Considering that K_d and K_z are, respectively, equivalent to the volume anisotropy K_v and the interface term $2K_s/t$ in Eq. (1), in our model r is a function of K_{eff} . Micromagnetic simulations (OOMMF code¹⁷) were performed to verify the model validity. We obtained the ground state configuration for 0.25, 0.5, 0.75, 1, and 2 μm diameter disks of a single Co layer as a function of the perpendicular anisotropy constant (K_z). The cell size was taken as $2 \times 2 \times 2$ nm³; $A=30 \times 10^{-12}$ J/m and $M_s=1400 \times 10^3$ A/m (the values used for bulk Co). Again, we have considered only the perpendicular term in the simulations; r was determined from a pseudo-Voigt function fit to $m_z(\rho)$ obtained from the simulation.

Our simulations (Fig. 1) show vortices when K_z is included, pointing to the possibility of obtaining vortices in Co/Pt multilayer disks. A more relevant conclusion is that r varies as a function of K_z , following the behavior predicted by our model [Eq. (3)]. A phase diagram (Fig. 1) displays core size versus K_z (and therefore Co thickness) for $D=250$, 500, 750, 1000, and 2000 nm [Eq. (3) is also plotted]. A good agreement between the core diameters is obtained for the simulation and our model [Eq. (3)] for all disk diameters investigated. From this phase diagram, we can distinguish three regimes. For low values of K_z (region I, Fig. 1), we find an ordinary vortex structure with nearly the expected vortex core diameter (~ 10 nm) for a soft magnetic micrometric disk, i.e., for $K_z=0$ [I-a in Fig. 1]. In region I, we observe a monotonic increase in the diameter as a function of K_z , as predicted by the model. The increase in $2r$ is extended up to the limit of validity given by Eq. (3) [I-b of Fig. 1], followed by region II in the graph of Fig. 1. In region II, we observe that by augmenting the interface contribution, the spin con-

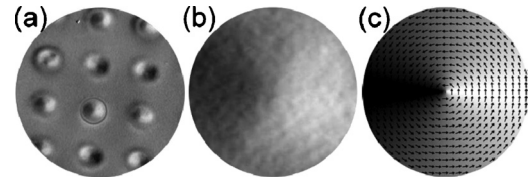


FIG. 2. (a) Image obtained by XMCD-PEEM of the $[\text{Co}_2/\text{Pt}_2] \times 6$ 1 μm disk array. (b) Detail of the disk highlighted by the red circle, presenting a typical vortex pattern. (c) OOMMF simulation of a disk with the same characteristic, showing a good agreement with (a).

figuration may present increasingly out-of-plane components. Besides the perpendicular magnetization of the vortex core, a perpendicular magnetization also appears at the rim of the disks [II-c in Fig. 1], forming a domain configuration of out-of-plane concentric rings. Although K_v is still larger than $2K_s/t$, the boundary conditions impose an out-of-plane K_{eff} . Region III: for $2K_s/t > K_v$, it gives rise to an out-of-plane single domain [region III and III-d of Fig. 1], and therefore the vortex is no longer observed.

Four samples, consisting of lithographed arrays of Co/Pt multilayered disks [$D=1$ and 2 μm] deposited by sputtering on $\text{SiO}_2/\text{Si}(100)$ wafers, were produced. Their structure was $([\text{Co}_t/\text{Pt}_2]_6/\text{Pt}_6)$ with Co layer thickness $t=2.0, 1.6, 0.8,$ and 0.6 nm. Continuous films were also produced in the same sputtering runs. The magnetic properties and morphology of the samples were characterized by magnetometry, x-ray magnetic circular dichroism (XMCD) photoelectron emission microscopy (PEEM) and magnetic force microscopy.

The XMCD-PEEM measurements were performed at the Nanospectroscopy beamline at Elettra Synchrotron, Italy. The final pictures were obtained by averaging up to 250 images (taken at Co L_3 edge) originated from subtracting two images acquired with opposite (left/right) circular polarizations. This imaging technique contrasts the magnetization alignment relative to the x-ray beam direction. The experiment was carried out in grazing incidence setup (16°), therefore the images distinguish mostly the in-plane magnetization distribution, the black/white contrast referring to parallel/antiparallel relation between the magnetization components and the beam direction. However, the measurements are still sensitive to the perpendicular magnetization, due to the angle between the perpendicular magnetization and the x-ray beam.

Figure 2 shows images of the $[\text{Co}_2/\text{Pt}_2] \times 6$ multilayered disks, which presented the highest K_{eff} . For the 1 and 2 μm array, almost all disks have a single vortex structure. This is confirmed if we compare the experimental result of a particular disk size with the equivalent simulated one (Fig. 2). The realization of magnetic vortices in a multilayer system represents a great step toward better controlling the magnetic vortex properties and characteristics.

For the arrays with a smaller Co thickness $[\text{Co}_t/\text{Pt}_2] \times 6$ ($t=0.6$ and 0.8 nm), i.e., for $K_{\text{eff}} \sim 0$, the magnetic configurations do not seem to correspond to an usual vortex [XMCD-PEEM image in Fig. 3(a)]. In this case, it is observed a smaller bright/dark contrast close to the center. Our interpretation is that we have the same spin configuration of region II of the phase diagram [see II-c in Fig. 1], i.e., at the center M is pointing upwards, at the rim downwards and in-between there is a planar vortex. For comparison, Fig. 3(b) also presents the spin configuration of c(II) (Fig. 1), but

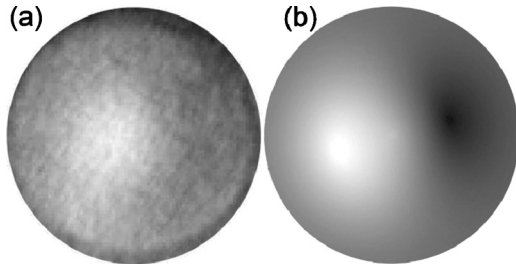


FIG. 3. (a) XMCD-PEEM image of $1 \mu\text{m}$ $[\text{Co}_{0.6}/\text{Pt}_2] \times 6$ disk. (b) simulated spin configuration of a disk of the same size (region II in the phase diagram of Fig. 1), showing a good agreement with (a).

in a pattern that mimics the PEEM contrast, showing a good agreement between the measurement and the simulation. In this case, the faint contrast is due to the 16° tilt angle between the plane of the sample and the x-rays direction.

Although the XMCD-PEEM technique is not well suited for assessing r , we could observe a behavior that corroborates our proposition. For the thicker Co layers, where it is expected a larger in-plane anisotropy, we obtained a vortex structure (Fig. 2). As we get closer to the spin reorientation transition condition, i.e., for thinner Co layers, we observed out-of-plane magnetization in concentric annular regions (Fig. 3). This agrees with the simulations, i.e., vortex structure and annular arrangement, corresponding to regions I and II (Fig. 1).

These results open up opportunities for optimizing VSTNOs devices.⁶ The magnetic dipole moment of the vortex core is proportional to its square radius (r); $\mu = \pi r^2 t M_s$. The synchronization of the gyrotropic motion of the cores in an array of vortices⁶ is dependent on the coupling between vortices through the antivortices, and therefore dependent on the dipolar and long-range exchange interactions between vortices and antivortices counter balanced by the restoring forces (Oersted field). Since both interactions depend on r , tailoring r is relevant for increasing the microwave power and for achieving phase locking in VSTNOs.

Maybe the most significant contribution of multilayer-based vortex systems would be the establishment of an alternative architecture for the VSTNOs, i.e., a vertical vortices stacking, possibly solving the problems of synchronization and power. This vortices stacking device is naturally phase-locked, since it is well-known that the Co layers are coupled,¹⁸ and therefore the power generated will be amplified relative to an individual vortex. Hence, we would have a

synchronized set of vortices in a very compact device.

In conclusion, tailoring magnetic vortex core diameters as well as other properties of magnetic disks is proposed by adjusting the interface energy contribution in Co/Pt multilayered structured system. The proposal is supported by a model and by micromagnetic simulations which present consistent results. Theory and simulation are also presented in the form of a phase diagram defining three regions with distinct domain structure. We demonstrated experimentally vortex formation on Co/Pt multilayered disks. We also verified that vortex nucleation is affected by the interface contribution, consistently with the model. Finally, we proposed and demonstrated a strategy to engineer magnetic vortex properties to suit technological application demands.

We thank FAPESP, CNPq, FAPERJ, LNLS, and Elettra for financial support.

- ¹A. P. Guimarães, *Principles of Nanomagnetism* (Springer, Berlin, 2009).
- ²C. L. Chien, F. Q. Zhu, and J.-G. Zhu, *Phys. Today* **60**(6), 40 (2007).
- ³S.-K. Kim, K.-S. Lee, Y.-S. Yu, and Y.-S. Choi, *Appl. Phys. Lett.* **92**, 022509 (2008).
- ⁴S. Bohlens, B. Krüger, A. Drews, M. Bolte, G. Meier, and D. Pfannkuche, *Appl. Phys. Lett.* **93**, 142508 (2008).
- ⁵D.-H. Kim, E. A. Rozhkova, I. V. Ulasov, S. D. Bader, T. Rajh, M. S. Lesniak, and V. Novosad, *Nature Mater.* **9**, 165 (2010).
- ⁶A. Ruotolo, V. Cros, B. Georges, A. Dussaux, J. Grollier, C. Deranlot, R. Guillemet, K. Bouzouane, S. Fusil, and A. Fert, *Nat. Nanotechnol.* **4**, 528 (2009).
- ⁷D. V. Berkov and N. L. Gorn, *Phys. Rev. B* **80**, 064409 (2009).
- ⁸R. Lehdorff, D. E. Bürgler, S. Gliga, R. Hertel, P. Grünberg, C. M. Schneider, and Z. Celinski, *Phys. Rev. B* **80**, 054412 (2009).
- ⁹D. Houssameddine, U. Ebels, B. Delaet, B. Rodmacq, I. Firastrau, F. Ponthenier, M. Brunet, C. Thirion, J.-P. Michel, L. Prejbeanu-Buda, M.-C. Cyrille, O. Redon, and B. Dieny, *Nature Mater.* **6**, 447 (2007).
- ¹⁰M. M. Soares, E. De Biasi, L. N. Coelho, M. C. dos Santos, F. S. de Menezes, M. Knobel, L. C. Sampaio, and F. Garcia, *Phys. Rev. B* **77**, 224405 (2008).
- ¹¹T. S. Machado, T. G. Rapoport, and L. C. Sampaio, *Appl. Phys. Lett.* **93**, 112507 (2008).
- ¹²M. T. Johnson, P. J. H. Bloemen, F. J. A. den Broeder, and J. J. de Vries, *Rep. Prog. Phys.* **59**, 1409 (1996).
- ¹³F. Garcia, F. Fettar, S. Auffret, B. Rodmacq, and B. Dieny, *J. Appl. Phys.* **93**, 8397 (2003).
- ¹⁴B. G. Park, J. Wunderlich, D. A. Williams, S. J. Joo, K. Y. Jung, K. H. Shin, K. Olejnik, A. B. Shick, and T. Jungwirth, *Phys. Rev. Lett.* **100**, 087204 (2008).
- ¹⁵J.-H. Park, M. T. Moneck, C. Park, and J.-G. Zhu, *J. Appl. Phys.* **105**, 07D129 (2009).
- ¹⁶P.-O. Jubert and R. Allenspach, *Phys. Rev. B* **70**, 144402 (2004).
- ¹⁷M. J. Donahue and D. G. Porter, <http://math.nist.gov/oommf/>.
- ¹⁸J. Moritz, F. Garcia, J. C. Toussaint, B. Dieny, and J. P. Nozières, *Europhys. Lett.* **65**, 123 (2004).